Electrodynamics of the antiferromagnetic state in URu_2Si_2

Jesse S. Hall, M. R. Movassagh, M. N. Wilson, G. M. Luke,* and T. Timusk*
Department of Physics and Astronomy, McMaster University, Hamilton, ON L8S 4M1, Canada

N. Kanchanavatee, M. Janoschek, N. P. Butch, and M. B. Maple
University of California San Diego, La Jolla, California, United States
(Dated: May 28, 2015)

We present data on the optical conductivity of $URu_{2-x}(Fe,Os)_xSi_2$. While the parent material URu_2Si_2 enters the enigmatic hidden order state below 17.5 K, an antiferromagnetic state is induced by doping Fe or Os onto the Ru sites. We find that both the HO and the AFM states exhibit an identical gap structure that is characterized by a loss of conductivity below the gap energy with spectral weight transfered to a narrow fequency region just above the gap, the typical optical signature of a density wave. The AFM state is marked by strong increases in both transition temperature and the energy of the gap associated with the transition. In the normal state just above the transition the optical scattering rate varies as ω^2. We find that in both the HO and the AFM states, our data are consistent with elastic resonant scattering of a Fermi liquid. This indicates that the appearance of a coherent state is a necessary condition for either ordered state to emerge. Our measurements favor models in which the HO and the AFM states are driven by the common physics of a nesting-induced density wave gap.

The heavy fermion metal URu_2Si_2 has a rich phase diagram in both temperature and pressure [1–3]. Uniquely among heavy fermion materials, as the temperature is lowered, the development of the heavy fermion state is interrupted by a second order phase transition at 17.5 K [4, 5] to an enigmatic "hidden order" state (HO). Despite intense experimental investigation [6–10] and proposed theoretical models [11–14], the nature of the phase transition has remained elusive.

When hydrostatic pressure is applied to the URu_2Si_2 the temperature of the transition rises steadily with pressure up to 20 K at 1.5 GPa,[15] at which point a first-order phase transition from the HO state with a small extrinsic magnetic moment [3, 16] to a large moment long-range antiferromagnetic (AFM) state [1, 17, 18] occurs. As the pressure is further increased the transition temperature continues to rise up to nearly 30 K [19]. Much attention has been placed upon the antiferromagnetic phase because quantum oscillation measurements [10] suggest that the Fermi surface does not change between the HO and AFM states. This allows calculations of the bandstructure [20, 21] and the Fermi surface, which can be computed for the AFM state, to be applied to the HO state.

Recently [22–24], it has been found that doping URu_2Si_2 with Fe onto the ruthenium sites can also induce antiferromagnetism in the system. Increasing the dopant concentration increases the transition temperature and, as with applied hydrostatic pressure, there is a crossover into antiferromagnetism above a certain doping level. The similarity of the phase diagrams with pressure and Fe doping suggests that the AFM states are equivalent. Doping with Os also induces an AFM state that raises the transition temperature [25]. In this paper, we present optical conductivity data on URu_2Si_2 in the doping-induced antiferromagnetic state and we report the first observations of the behavior of the energy gap for charge excitations in the AFM state and its evolution with increasing doping.

Samples of URu_2Si_2 were grown in a tri-arc furnace in an argon atmosphere. Doping levels were controlled by mixing stoichiometric amounts of the reagents and confirmed using x-ray powder diffraction. Magnetic transitions were characterized using a SQUID magnetometer and the antiferromagnetic moment was measured separately using muon spin resonance [24]. DC resistivity measurements were performed in an Oxford Maglab PPMS using a four-probe geometry; the estimated error due to sample configuration and geometry is 20%, which is consistent with the variation in measurements in the literature [4, 26]. Optical measurements were performed using an SPS 200 Martin-Puplett Fourier-transform interferometer for reflectance measurements below 20 meV and a Bruker IFS 66v/s FTIR spectrometer for measurements from 15 meV to 4.5 eV. Absolute reflectance was obtained using a standard gold evaporation technique[27], and the optical conductivity was obtained by performing Kramers-Kronig analysis on the absolute reflectance data.

Figure 1 shows the absolute reflectance of $URu_{2-x}(Fe,Os)_xSi_2$ in the AFM state (panes a) and b)) and at different dopant concentrations x for Fe doping (panel c)) and for Os doping (panel d)). The undoped parent compound with $x = 0$, which is in the HO state, is shown as well. In all curves a single strong minimum develops as the temperature is lowered below the transition. As the doping is increased the reflectance minimum moves to higher frequencies.

The characteristic absorption that signifies the opening of the HO gap in the parent compound is still present in

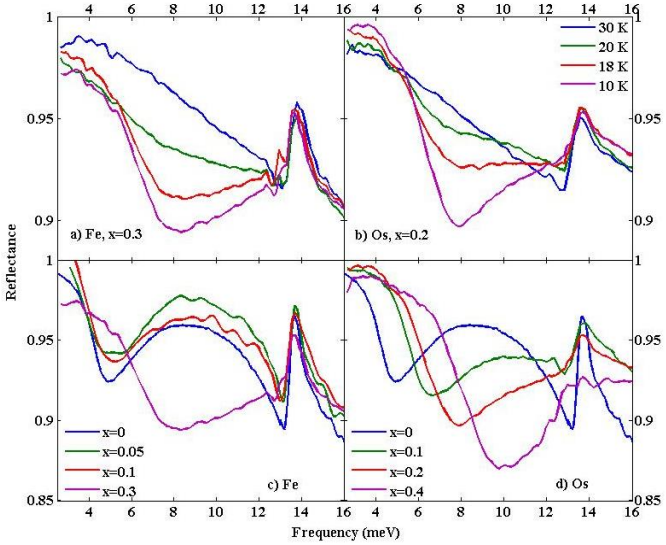

FIG. 1. Temperature and doping dependence of the reflectance of doped samples of $URu_{2-x}(Fe,Os)_xSi_2$. The top panels shows the absolute reflectance for a) Fe doping, b) Os doping, both in the AFM state as a function of temperature. The bottom panels show the absolute reflectance as function of doping for c) Fe doping and d) Os doping. The prominent depression of reflectance that develops in the 5 to 10 meV region in all the samples is a signature of a gap in the density of states. Doping with Fe and Os causes the reflectance minimum to move to higher frequency but the signature of the gap, a single minimum of reflectance, does not change with doping.

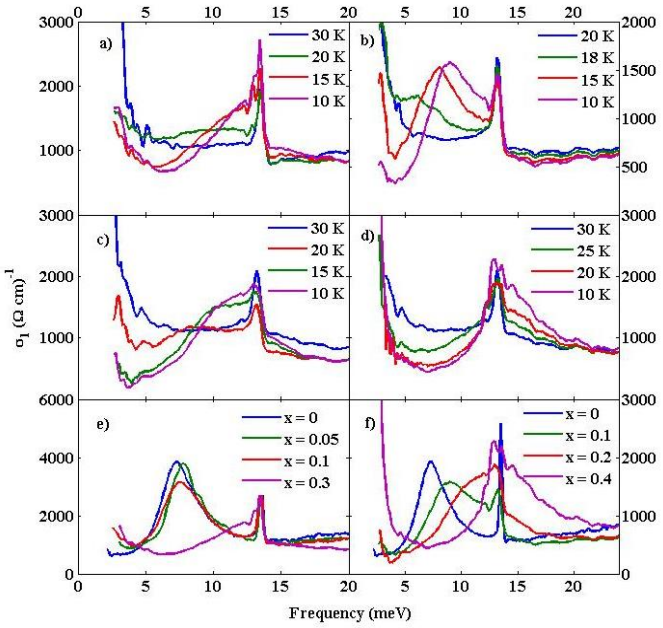

FIG. 2. Optical conductivity of $URu_{2-x}(Fe,Os)_xSi_2$ in the antiferromagnetic state. Panels a) to d) show the optical conductivity changes with temperature. The dopants and concentrations are a)Fe x=0.3, b)Os x=0.1, c)Os x=0.2, and d)Os x=0.4. Panel e) shows the dependence of the conductivity on the dopant concentration for Fe doping, with the parent material shown for comparison; panel f) shows the same for Os doping. The parent compound conductivities have been reduced by a factor of 0.5? to allow easier comparison.

the AFM state, remarkably unchanged except for a shift to higher energies. There is no evidence of a second, different gap due the AFM state. Previously [28] we have shown that when two gaps are present in URu_2Si_2, as in the case of the c-axis conductivity, it is possible to see the characteristic change in the absorption due to this effect. The absence of a second gap here strongly argues for a common gap-forming mechanism in the HO and AFM states. The data in Figure 1 also shows that the phonon peaks at 13.6 meV do not shift in energy with doping.

Figure 2 shows the AC conductivity of $URu_{2-x}(Fe,Os)_xSi_2$. In the paramagnetic state, above the HO and AFM transition temperatures, the conductivity consists of a Drude peak and an incoherent continuum. As in the undoped sample [28], the continuum develops a gap-like minimum which is unaltered in overall character between the HO to the AFM state: there is a characteristic depletion of spectral weight in the gap region followed by a recovery in the frequency range immediately above the gap. The Drude peak that develops in the hybridization regime narrows but is otherwise unaffected by the emergence of the ordered states. The principal effect of Os and Fe doping is an increase in the energy of the gap, in tandem with the increase in transition temperature. In the Os-doped samples, the 13.6 meV phonon disappears at higher dopings and lower temperatures, while in the Fe-doped sample it remains on top of the "hump" where spectral weight is recovered.

We can characterize the gap Δ using a simple formula for a square root singularity in the density of states as we have done previously for the parent material [28], giving a reasonable estimate for the size of the gap and its temperature evolution. This is shown in Table 1. The ratio $2\Delta/k_BT_0$ has two values, a lower value of 4.2 in the HO state and a somewhat higher value of 5.2 in the AFM state. The charge gap closely tracks the transition temperature in both the AFM and HO states, regardless of the dopant used to induce antiferromagnetism. In particular, the value of $2\Delta/k_BT_0$, where T_0 is the transition temperature to the ordered state (HO or AFM), is the same in the normal state for the parent compound and for the Fe doped material, and has nearly the same value in the AFM state for both Fe doping and Os doping at all dopant concentrations measured. This clearly demonstrates that the AFM state is the same for all samples and is not specific to the dopant used.

It is worth comparing these results to those obtained by other techniques in the antiferromagnetic state. Resistivity measurements on URu_2Si_2 performed under pressure

Fe	Δ meV	T_0 K	$2\Delta/k_BT_0$	phase
x = 0	3.2	17.5	4.23	HO
x = 0.05	3.32	18.2	4.23	HO
x = 0.1	3.43	18.5	4.28	HO
x = 0.3	5.14	23	5.20	AFM
Os	Δ meV	T_0 K	$2\Delta/k_BT_0$	phase
x = 0	3.2	17.5	4.23	HO
x = 0.1	4.35	19.5	5.17	AFM
x = 0.2	5.14	23	5.19	AFM
x = 0.3	6.64	29	5.31	AFM

TABLE I. Gap values for the various levels of doping by Fe and Os. The gap and the critical temperature increase monotonically with doping. The $2\Delta/k_BT_0$ ratio is constant at 4.2 in the HO state and 5.2 in the AFM state.

by Jeffries *et al.* [29] and with Fe doping by Das *et al.* [23] suggest that, as the transition temperature rises, the gap remains constant in the HO state, then rises to higher values in the AFM state. In contrast, our measurements clearly show that the gap in the electronic density of states at the Fermi level tracks the rising transition temperature in both the HO and AFM states. There is a small jump at the crossover before a smooth continuous rise in the gap energy with doping.

We now turn to the excitations in the paramagnetic normal state above the ordered HO and AFM states. As in the HO state, in the AFM state below 70 K the conductivity in the 5 meV to 40 meV region decreases monotonically with decreasing temperature forming the so-called "hybridization gap"[30]. The spectral weight lost is transferred to much higher frequencies[31, 32] while both HO and AFM states shift the spectral weight lost in the gap to a new hump feature immediately above the gap. Another common feature of the HO and AFM states is the "arrested hybridization". In both states the hybridization gap stops changing below the HO/AFM transition temperature.

Figure 3 shows the scattering rate as a function of frequency for undoped URu_2Si_2 in the normal state above the hidden order transition. At 30 K the the scattering rate varies linearly with frequency *i.e.* non Fermi liquid like. At 20 K coherence has developed with $1/\tau < \omega$ and the scattering rate varies as ω^2. We show that with doping the same behavior obtains, the ordered state, regardless of the order parameter, always emerges from a Fermi liquid precursor. This fact is not immediately apparent from transport measurements alone as the Fermi liquid temperature range is too narrow to establish a conventional T^2 dependence; it is only by looking at the optical scattering rate that it becomes clear that this must be the case.

Figure 4 shows the AC resistivity as a function of ω^2 for the doped compounds at temperatues just above the phase transition to the ordered state. It is linear

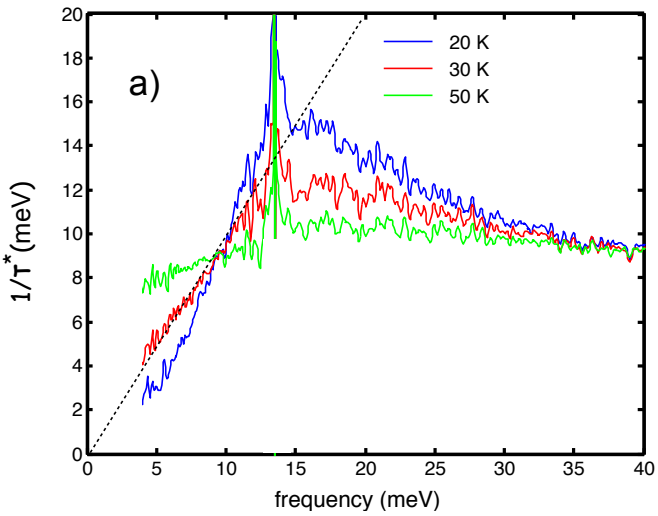

FIG. 3. Scattering rate of the parent compound is linear with frequency above 30 K but develops an ω^2 dependence below a temperature where coherence sets in (dashed line) [30]. We note that in the doped compound the Fermi liquid region has moved up in temperature to 30 K as shown in Fig.4.

in the low frequency regime $\omega \lesssim 8.5$ meV, indicating quadratic dependence of the scattering rate on frequency. This is true at temperatures well above the range where quadratic scattering rates are observed in the parent compound, indicating that $URu_{2-x}(Fe,Os)_xSi_2$ is a coherent (though anomalous [30, 33], see below) Fermi liquid in the normal state in a narrow temperature range above the transition regardless of whether the transition is to the HO or the AFM state.

For a Fermi liquid, in addition to the ω^2 frequency dependence, one also expects a T^2 temperatuere dependence of the resistivity. It was shown that the full resistivity is given by [34, 35]:

$$\rho(\omega, T) = C(\omega^2 + b\pi^2 T^2) \quad (1)$$

where the value of the coefficient C depends on the band structure but $b = 4$ for umklapp scattering [35] independent of the details of a particular material. It was pointed out recently that for many strongly correlated systems the b coefficient varied from 1.0 up to 2.5 and in particular for URu_2Si_2 it had a value of $b = 1.0$ in a narrow range of temperatures above the hidden order transition [30]. Malsov and Chubukov showed that this anomalous behavior can be the result of resonant elastic scattering [35]. In the case at hand the scattering centers would be the unhybridized f electrons.

Figure 5 shows the DC resistivity and its temperature derivative for $URu_{2-x}(Fe,Os)_xSi_2$. The resistivity bears many of the hallmarks of the resistivity of the parent compound [30], with the transition marked by the same "mogul-like" feature that shifts up in temperature with doping. The first derivative of the resistivity is charac-

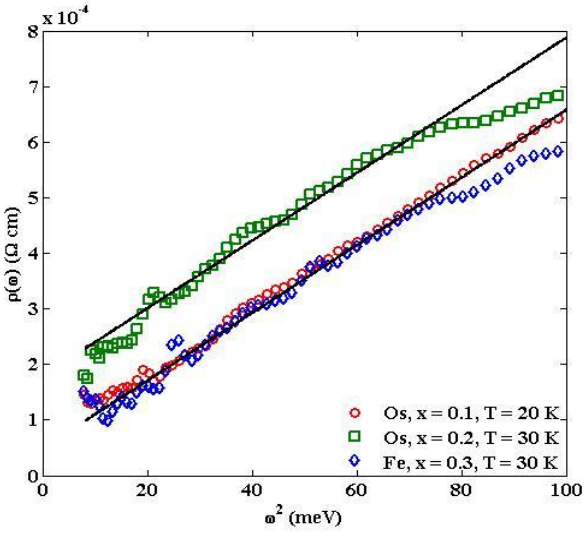

FIG. 4. The optical resistivity is linear when plotted against the square of the frequency. The closer to the transition the temperature at which $\rho(\omega)$ is measured, the higher in frequency the linear fit is valid. In all samples, regardless of the temperature of the transition or whether it was to an AFM or HO state, the scattering is quadratic frequency immediately above the transition, the same behavior that is seen in the parent compound [30]. As the transition temperature rises with doping, the temperature at which Fermi liquid behavior appears rises as well.

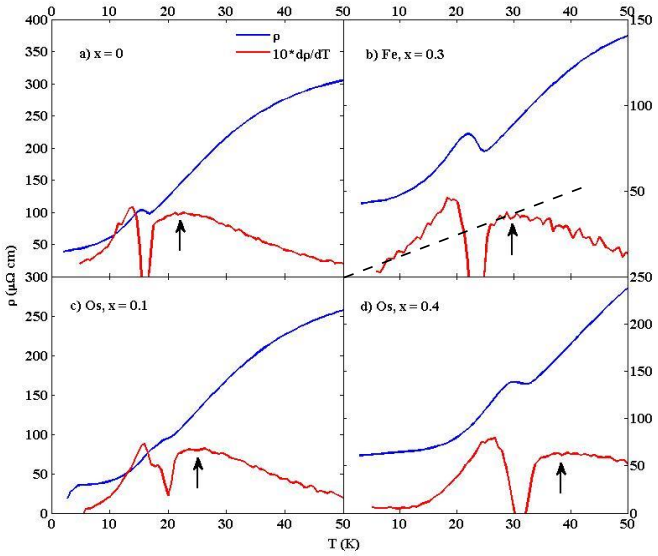

FIG. 5. The DC resistivity and its first derivative for $URu_{2-x}(Fe,Os)_xSi_2$. The transition at T_0 to the ordered state is marked by a sudden sharp minimum in the resistivity.The resistivity of the parent compound has the same hallmarks as that of the doped material. As the transition is approached from above the derivative reaches a maximum indicated by arrows in the figure, that always precedes the transition. The effect of doping is to move the whole structure to higher temperatues preserving its overall features. The dashed line denotes Femi liquid behavior where $d\rho(T)/dT = 2AT$

terized by a broad asymmetric peak above the transition. The transition itself is signaled as a sudden sharp drop in the derivative to negative values. With increased doping this pattern shifts upwards in temperature. It is noteworthy that the turnover in the derivative has the same character in samples with a HO transition and those with an AFM transition. This is analogous to the behavior of the resistivity under pressure [29].

Because the temperature range of Fermi liquid behavior is the narrow region between onset of coherence and the transition to the ordered state, we cannot use the usual method of plotting $\rho(T) = AT^2$ to determine the coefficient A and then from it b. Instead we adopt the following procedure. Assuming that Eq. 1 holds we can determine C from the slope of the frequency dependence as shown in Fig. 4. To find A we draw a straight line from the experimental resistivity derivative line to the origin as shown in Fig. 5b (dashed line), in effect assuming that $d\rho/dT = 2AT$ where, in our notation, $A = Cb\pi^2$. Using this procedure we find that in the normal state at 19 K $b = 1.1$ in the parent compound, while for the Fe $x = 0.3$ material, just above the AFM transition at 30 K, $b = 1.35$. So, in both materials, above the transition, there is a coherent Fermi liquid with anomalous b. At the same temperature, in the undoped material, the frequency dependence is not Fermi liquid like and the transport is incoherent i.e. $1/\tau > \omega$. Thus we conclude that chemical pressure moves both the second order transition temperature and the region where we observe coherent ω^2 Fermi liquid behavior in concert to higher temperatures.

This observation indicates that regardless of the nature of the transition (AFM or HO) or the temperature at which it occurs, the dominant scattering mechanism for the charge carriers is due to scattering of coherent quasiparticles from resonant impurities. This was previously shown [30] to be the case for the parent material. We conclude that the emergence of this anomalous Fermi liquid scattering is a precondition for the occurrence the ordered state. Coherence and a well developed Femi surface are necessary conditions for a nesting induced density wave. What we *not* observed in the normal state in URu_2Si_2 is scattering by discrete bosonic excitations. (For exampe the 41 meV magnetic resonance in the cuprates[36]).

In summary we have studied two ordered states of URu_2Si_2 spectroscopically: the hidden order state and the antiferromagnetic state. The two states show few differences other than an overall smooth increase in the gap and the transition temperature with chemical pressure. In the ordered states the the gap and the transfer of spectral weight are characteristic of density waves. The normal states are also very similar: they are Fermi liquid like with a scaling factor $b \approx 1.0$ characteristic of a Fermi

liquid dominated by resonant impurity scattering. That state develops at higher temperatures in the doped samples is not surprising: under chemical pressure the unit cells are smaller increasing hybridization and raising the temperature where coherence is possible. Model that include nesting-induced density waves are consistent with our observations: efficient nesting is promoted by coherent well-defined Fermi surfaces.

We thank P. Coleman, G. Kotliar, D.L. Maslov, S.S. Lee, B.D. Gaulin, D. Maslov, A.M. Tremblay, for helpful discussions. This work was supported by the Natural Science and Engineering Research Council of Canada and by the Canadian Institute for Advanced Research.

* Canadian Institute for Advanced Research

[1] H. Amitsuka, M. Sato, N. Metoki, M. Yokoyama, K. Kuwahara, T. Sakakibara, H. Morimoto, S. Kawarazaki, Y. Miyako, and J. A. Mydosh, Phys. Rev. Lett. **83**, 5114 (1999).
[2] F. Bourdarot, A. Bombardi, P. Burleta, M. Enderlec, J. Flouquet, P. Lejay, V. M. N. Kernavanoisc, L. Paolasinib, M. Zhitomirskya, and B. Fak, Physica B **359-361**, 986 (2005).
[3] K. Matsuda, Y. Kohori, T. Kohara, H. Amitsuka, K. Kuwahara, and T. Matsumoto, Journal of Physics: Condensed Matter **15**, 2363 (2003).
[4] T. T. M. Palstra, A. A. Menovsky, and J. A. Mydosh, Phys. Rev. B **33**, 6527 (1986).
[5] M. B. Maple, J. W. Chen, Y. Dalichaouch, T. Kohara, C. Rossel, M. S. Torikachvili, M. W. McElfresh, and J. D. Thompson, Phys. Rev. Lett. **56**, 185 (1986).
[6] C. R. Wiebe, J. A. Janik, G. J. MacDougall, G. M. Luke, J. D. Garrett, H. D. Zhou, Y.-J. Jo, L. Balicas, Y. Qiu, J. R. D. Copley, Z. Yamani, and W. J. L. Buyers, Nature Phys. **3**, 96 (2007).
[7] A. F. Santander-Syro, M. Klein, F. L. Boariu, A. Nuber, P. Lejay, and F. Reinert, Nature Phys. **5**, 637 (2009).
[8] A. R. Schmidt, M. H. Hamidian, P. Wahl, F. Meier, A. V. Balatsky, J. D. Garrett, T. J. Williams, G. M. Luke, and J. C. Davis, Nature **465**, 570 (2010).
[9] P. Aynajian, E. H. da Silva Neto, C. V. Parker, Y.-K. Huang, A. Pasupathy, J. A. Mydosh, and A. Yazdani, PNAS **107**, 10383 (2010).
[10] E. Hassinger, G. Knebel, T. D. Matsuda, D. Aoki, V. Taufour, and J. Flouquet, Phys. Rev. Lett. **105**, 216409 (2010).
[11] K. Haule and G. Kotliar, Nat. Phys. **5**, 796 (2009).
[12] Y. Dubi and A. V. Balatsky, Phys. Rev. Lett. **106**, 086401 (2011).
[13] P. Chandra, P. Coleman, and R. Flint, Nature **493**, 621 (2013).
[14] P. S. Riseborough, B. Coqblin, and S. Magalhaes, Physical Review B **85**, 165116 (2012).
[15] M. W. McElfresh, J. D. Thompson, J. O. Willis, M. B. Maple, T. Kohara, and M. S. Torikachvili, Phys. Rev. B **35**, 43 (1987).
[16] P. G. Niklowitz, C. Pfleiderer, T. Keller, M. Vojta, Y.-K. Huang, and J. A. Mydosh, Phys. Rev. Lett. **104**, 106406 (2010).
[17] H. Amitsuka, K. Matsuda, I. Kawasaki, K. Tenya, M. Yokoyama, C. Sekine, N. Tateiwa, T. Kobayashi, S. Kawarazaki, and H. Yoshizawa, Journal of Magnetism and Magnetic Materials **310**, 214 (2007).
[18] F. Bourdarot, S. Raymond, and L.-P. Regnault, Philosophical Magazine **94**, 3702 (2014).
[19] E. Hassinger, G. Knebel, K. Izawa, P. Lejay, B. Salce, and J. Flouquet, Physical Review B **77**, 115117 (2008).
[20] S. Elgazzar, J. Rusz, M. Amft, P. M. Oppeneer, and J. A. Mydosh, Nature Materials **8**, 337 (2009).
[21] P. M. Oppeneer, S. Elgazzar, J. Rusz, Q. Feng, T. Durakiewicz, and J. A. Mydosh, Phys. Rev. B **84**, 241102 (2011).
[22] N. Kanchanavatee, M. Janoschek, R. E. Baumbach, J. J. Hamlin, D. A. Zocco, K. Huang, and M. B. Maple, Phys. Rev. B **84**, 245122 (2011).
[23] P. Das, N. Kanchanavatee, J. S. Helton, K. Huang, R. E. Baumbach, E. D. Bauer, B. D. White, V. W. Burnett, M. B. Maple, J. W. Lynn, and M. Janoschek, Phys. Rev. B **91**, 085122 (2015).
[24] M. N. Wilson and G. M. Luke, In preparation (2015).
[25] N. Kanchanavatee, B. White, V. Burnett, and M. Maple, Philosophical Magazine **94**, 3681 (2014).
[26] J. R. Jeffries, N. P. Butch, B. T. Yukich, and M. B. Maple, Phys. Rev. Lett **99**, 217207 (2007).
[27] C. C. Homes, M. Reedyk, D. Cradles, and T. Timusk, Applied optics **32**, 2976 (1993).
[28] J. S. Hall, U. Nagel, T. Uleksin, T. Rõõm, T. Williams, G. Luke, and T. Timusk, Phys. Rev. B **86**, 035132 (2012).
[29] J. R. Jeffries, N. P. Butch, B. T. Yukich, and M. B. Maple, J. Phys. Cond. Matt. **20**, 095225 (2008).
[30] U. Nagel, T. Uleksin, T. Rõõm, R. P. S. M. Lobo, P. Lejay, C. C. Homes, J. Hall, A. W. Kinross, S. Purdy, T. J. Williams, G. M. Luke, and T. Timusk, PNAS **109**, 19161 (2012).
[31] W. T. Guo, Z. G. Chen, T. J. Williams, J. D. Garrett, G. M. Luke, and N. L. Wang, Phys. Rev. B **85**, 195105 (2012).
[32] J. S. Hall and T. Timusk, Phil. Mag. **94**, 3760 (2014).
[33] M. R. Movassagh, Master's thesis, McMaster University (2014).
[34] R. Gurzhi, Soviet Physics JETP **35**, 673 (1959).
[35] D. L. Maslov and A. V. Chubukov, Phys. Rev. B **86**, 155137 (2012).
[36] J. Hwang, T. Timusk, E. Schachinger, and J. Carbotte, Physical Review B **75**, 144508 (2007).